# Considerations on Quality Metrics for Self-localization Algorithms

Juergen Eckert[1], Felix Villanueva[2], Reinhard German[1], and Falko Dressler[1]

[1] Computer Networks and Communication Systems, Dept. of Computer Science, University of Erlangen, Martensstrasse 3, 91058 Erlangen, Germany
{juergen.eckert,german,dressler}@cs.fau.de
[2] Computer Architecture and Networks, School of Computer Science, University of Castilla-La Mancha, Paseo de la Universidad 4, 13071 Ciudad Real, Spain
felix.villanueva@uclm.es

**Abstract.** The demand for location awareness and, therefore, the demand for self-localization techniques is continuously increasing. As a result, a good number of systems and methods for self-localization have been developed. Almost every system described in the literature exploits specific hardware or scenario features to solve the positioning issue, e.g. by using anchor nodes, relying on distances or angles, and even focusing on quite different distances ranging from centimeters to several kilometers. In many cases, the metrics used to evaluate the localization quality have been chosen according to the scenario. In this paper, we thoroughly discuss the most frequently used metrics for evaluating the quality of self-localization techniques. According to our findings, careful handling of some commonly used metrics is strongly required. We further propose an area-based solution that is especially helpful to measure and to compare different localization systems, which only need exact localization in a local context independently from specific scenario or hardware requirements. In this paper, we try to shed light on the question how to compare those very different techniques. In particular, we suggest the use one of two attribute-independent metrics. The first one is a generalization of an already quite popular metric, the Global Energy Ratio (GER), and the latter, the Area Ratio (AR), is a new approach based on the covered area.

**Keywords:** Localization, quality metrics, sensor networks, self-organization.

## 1 Introduction

Location awareness and the related localization techniques have become one of the most important issues in the field of wireless networking and mobile computing. With the emergence of a new class of location-aware distributed applications, and with new developments in the area of massively distributed systems, localization techniques are even becoming a key factor influencing the quality of those

C. Bettstetter and C. Gershenson (Eds.): IWSOS 2011, LNCS 6557, pp. 104–115, 2011.

applications. Among others, Wireless Sensor Networks (WSNs) and Sensor and Actor Networks (SANETs) are in the main focus of self-localization, i.e. the capability of autonomously generating (relative) location information [2,4].

One of the biggest problems of providing this information is to generate a reference grid or a map in advance. No system is working without this very costly or complex effort. Pure manual generation is very costly whereas a (partial or full) autonomous generation tends to be erroneous. The distinction between pure localization clients and producers is in most cases not obvious. As the system is growing the producers are expanding it in relation to the previously established knowledge. If this initial step or some measurements are wrong then this resulting placement error is mostly propagated through large parts of the set-up.

There is a wide variety of those localization techniques available, using lateration, angulation, and scene analysis techniques [3,6,16]. Many of the algorithms described in the literature have been designed for a specific sensing method but do not perform well in other environments. Some of these solutions have even been defined in the context of a complete self-localization system. Obviously, each of the proposed localization techniques has been thoroughly evaluated – in many cases not relying on a commonly accepted metric. This makes it impossible to compare or makes it very hard to choose the appropriate localization technique for an application. To simplify the evaluation of different approaches it would here be useful to have a limited amount of metrics.

Recently, a number of different metrics have been proposed. Most of them are taking special hardware attributes, measurement distances, or connectivity ranges into account; others are not independent of the number of nodes. A survey of general problems of localization including the used metrics can be found in the book by Mao and Fidan [14].

In this paper, we try to cast light on the quality of the localization results. We first briefly introduce the most common metrics and discuss their advantages and drawbacks. The main contribution is the finding that some metrics produce misleading results for certain classes of algorithms or scenarios. Furthermore, we present an area-based metric that is especially useful when studying algorithms that mainly relay on the localization accuracy in a local context. Based on the provided recommendations, it is possible to select an adequate metric for a particular class of algorithms and scenarios.

The remainder of the paper is organized as follows. Section 2 briefly describes our application scenario and motivates the paper. In Section 3, we introduce and discuss selected quality metrics including our proposed AR. Finally, Section 4 concludes the paper.

## 2 Evaluation Setup

Our scenario is a completely self-organizing approach to create a stable reference grid similar to the work by Liu *et al.* [13] using autonomous robot systems. Such systems can explore unknown environments and, at the same time, span a reference grid for highly accurate indoor local. Figure 1 depicts the basis scenario,

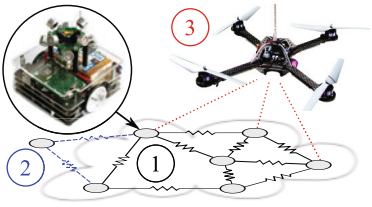


**Fig. 1.** Localization reference grid based on self-organizing robot systems

which we also used to describe our self-localization approach described in [5,6] Mobile nodes are autonomously deploying themselves on the ground forming a reference grid (step 1 in Figure 1). No global synchronization, knowledge, or state is available. Thus, nodes can arrive or depart from the system at any point in time (step 2 in Figure 1). A customer, e.g. a quadrocopter, can finally use the system to determine its current location (step 3 in Figure 1).

Our system relies on ultrasonic distance and (rough) angle measurements and supports accurate real-time localization of moving customers [7]. For more details on the scenario please refer to [8].

During the decision process of finding an appropriate method for creating and maintaining the reference system (step 1 in Figure 1), we observed that comparing different approaches is extremely challenging. Even the direct comparison of related algorithms is not possible in many cases: A lot of attributes have to be weighted against each other, accuracy and cost being the two primary ones.

Many researchers are creating their own evaluation scenario using hardware and scenario specific parameters, and are adapting some metric for the evaluation process. For comparison purposes, one would have to apply the very same parameters to a testbed, or would have to adjust the previous algorithms to work on the new hardware (or simulator). Both strategies may be very time consuming and even not be possible at all. Therefore, a common and widely accepted metric for comparison is needed, which is independent of any physical constrains such as the measurement technique, the network size, or the topology.

For the evaluation of different metrics, we implemented our fully distributed and self-organizing Mass-Spring-Relaxation (MSR) based technique [5,6] together with three different optimization steps of this algorithm in a simulation model. In the following, we use identifiers A1 to A4 to describe the different self-localization approaches: Algorithm A1 represents the classical MSR approach [11]. For Algorithm A2, variable node weights and an improved initial node positioning were introduced. Algorithm A3 features the capability of locally solving misplaced (flipped) node issues. Furthermore, the initial position is generated according to an existing network. Finally, Algorithm A4 introduces sector-of-arrival measurements in addition to the distance information. Details of these optimizations are out of the scope of this paper, please refer to [5,6]. As guideline, we can say that Algorithms A1 and A2 are performing rather poor, A3 performs quite good for small network sizes and, finally, Algorithm A4 performs nearly optimal for all tested network sizes.

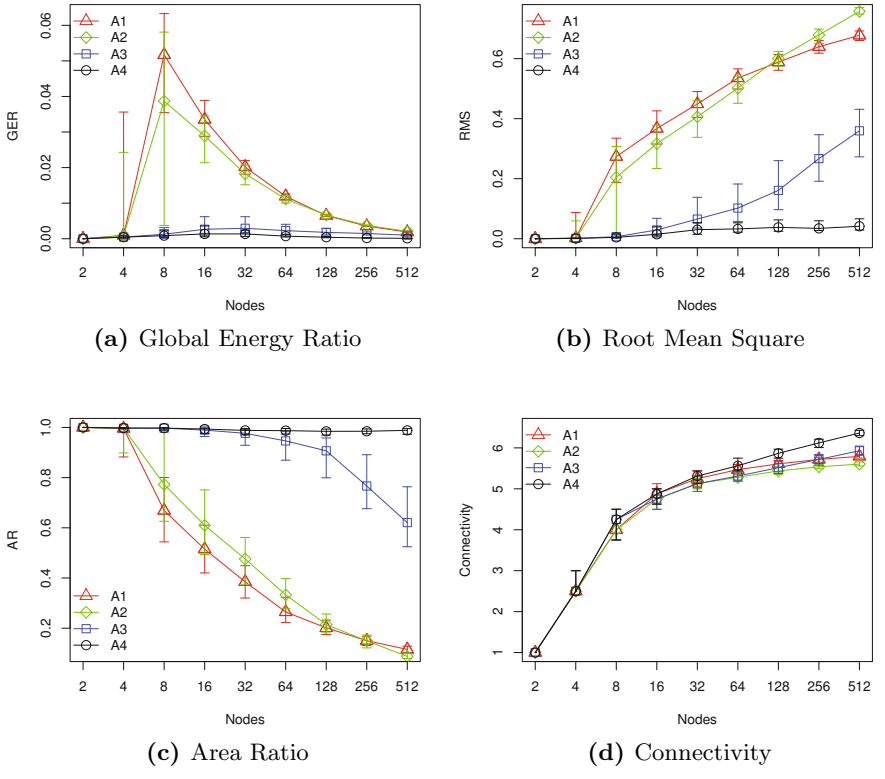


**(a)** Global Energy Ratio **(b)** Root Mean Square

**(c)** Area Ratio **(d)** Connectivity

**Fig. 2.** Selected simulation results

As depicted in Figure 2, we simulated different network sizes of 2 to 512 nodes. For statistical evidence, we executed 200 runs for each experiment in randomly chosen topologies. The presented plots show the median (50 % quantile). The error bars depict the stable co-domain (25 % and 75 % quantiles). The details of Figures 2a, 2b and 2c will be explained later in detail.

Figures 2a, 2b, and 2c depict the variation in quality of the different refinements. The specific characteristics of the metrics will be discussed in Section 3. Figure 2d shows the average connectivity of a node for the different network sizes and optimization steps. It can be seen that all algorithms have the same connectivity. However, connectivity in general is an important attribute for most localization algorithms. After reaching convergence, this value becomes less important for evaluating the achieved position accuracy.

## 3 Towards a Common Quality Metric

We assume that the network the localization approaches are implemented and evaluated on is represented by an underlaying connected graph $G = (V, E)$ with

vertex set $V$ and edge set $E$. Node $i$ is associated with the vertex $N_i \in V$. Neighbors are defined as nodes that can directly interfere (sense and/or communicate) with each other. Such a node pair $(i, j)$ is represented by an edge $(N_i, N_j) \in E$ in the graph. Two different mapping representations $p : V \rightarrow \Re^n$ for the underlying graph $G$ exist. The first representation $p_r$ is called *ground truth* and is defined as *a priori* knowledge of all physical node positions. Therefore it assigns a $\boldsymbol{x} \in \Re^n$ position tuple to a node ($\boldsymbol{x}_i = p_r(N_i)$). This knowledge is typically unknown to the algorithm but can easily be achieved within a simulator or within a controlled lab environment. The second representation $p_v$ is called *virtual coordinate system*. Its position tuples $\widehat{\boldsymbol{x}} \in \Re^n$ represent the result of the algorithm ($\widehat{\boldsymbol{x}}_i = p_v(N_i)$).

Quality metrics in the field of localization techniques shall help to identify how accurate a certain algorithm is able to reconstruct the ground truth. With the exception of a few metrics (e.g., [9]), most of the existing metrics rely on this information. Those few metrics are, due to the lack of global knowledge, not so reliable, however, quite useful for a real application. In this paper, we assume that ground truth can be obtained.

Both *absolute* and *relative* metrics have to be considered. Absolute metrics compare the estimated with the physical positions:

$$p_r(N_i) = p_v(N_i) + \boldsymbol{\epsilon}_i;\ \forall N_i \in V \tag{1}$$

This is only applicable if anchors with known positions $p_v(\cdot)$ are present. These are acting as interfaces between the real and the information driven virtual world. Otherwise, the generated localization grid might be arbitrarily shifted, rotated, or mirrored. Absolute position metrics cannot be applied without those interconnecting elements. In contrast, relative metrics can always be applied to any system, because only relative relationships are necessary, e.g. ($\|\cdot\|_p$ is an arbitrary distance norm):

$$\|p_r(N_i) - p_r(N_j)\|_p = \|p_v(N_i) - p_v(N_j)\|_p + \epsilon_{i,j};\ \forall N_i, N_j \in V \tag{2}$$

A generalized quality metric should be able to rely on such relative positions.

### 3.1 Distance Based Metrics

In 2003, Priyantha et al. [15] introduced a metric called the Global Energy Ratio (GER). The authors removed all hardware-specific or technique dependent attributes by computing a normalized error $\widehat{e}_{ij}$ between the $i$-th and the $j$-th node according to Equation 3 ($(N_i, N_j) \in E_{all}; E \subseteq E_{all} := \{(N_a, N_b) | \forall N_a, \forall N_b \in V\}$; i.e. a fully connected graph), where the distances $d_{ij}$ and $\widehat{d}_{ij}$ represent the true distance ($d_{ij} = \|p_r(N_i) - p_r(N_j)\|_2$) and the result of the algorithm ($\widehat{d}_{ij} = \|p_v(N_i) - p_v(N_j)\|_2$), respectively.

$$\widehat{e}_{ij} = \frac{\widehat{d}_{ij} - d_{ij}}{d_{ij}} \tag{3}$$

This error is then used for computing the GER as depicted in Equation 4, where $N$ represents the network size.

$$\mathrm{GER} = \frac{\sqrt{\sum_{i,j:i<j} \widehat{e}_{ij}^2}}{N(N-1)\frac{1}{2}} \tag{4}$$

Figure 2a depicts the plot of GER in our simulation results. As the network size increases, the values are getting smaller. This is certainly not the expected behavior: The real errors get larger with the number of nodes. This indicates that the resulting error is not independent of the network size for GER.

In 2005, Ahmed et al. [1] published a new metric called the Global Distance Error (GDE) where they tried to compensate this defect. The same normalized error $\widehat{e}_{ij}$ (Equation 3) is used again. However, for computing the GDE according to Equation 5, a normalization is added according to the connectivity range $R$. Thereby, the authors took more than position into concern, which is again not applicable for arbitrary comparison, e.g. no distance ranges are available for angulation techniques. We omit the plots of our simulation results in this paper; the results are comparable to those shown in Figure 2b, scaled by $\frac{1}{R}$.

$$\mathrm{GDE} = \frac{1}{R}\sqrt{\frac{\sum_{i,j:i<j} \widehat{e}_{ij}^2}{N(N-1)\frac{1}{2}}} \tag{5}$$

In 2005, Gotsman and Koren [10] presented the Average Relative Deviation (ARD) metric. Here, each distance error is treated equally. The calculation of the ARD is depicted in Equation 6. In contrast, the GER explicitly aims to give more weight to outliers, so that errors become quickly obvious. Thus, this arithmetic mean is not very suitable for accurate error metrics – even though the resulting plots are looking pretty much the same as those of Figure 2b due to nearly uniform error distribution of our obstacle-less simulator.

$$\mathrm{ARD} = \frac{2}{N(N-1)} \sum_{i,j:i<j} \frac{\widehat{d}_{ij} - d_{ij}}{min(\widehat{d_{ij}}, d_{ij})} \tag{6}$$

Based on the described metrics and the observations made in our experiments, we suggest to utilize the Root Mean Square (RMS) of the normalized error, which is actually a minor variation of GER and GDE. The key issue was the sensitivity of the GER to the number of nodes, which is no longer present for RMS. In addition, the metric is more influenced by outliers (as the ARD) to make it more descriptive for worst cases. RMS also relies in the normalized errors $\widehat{e}_{ij}$ (Equation 3) and weights those compared to the number of nodes $N$ in the network as shown in Equation 7. The plot in Figure 2b shows monotone increasing functions. This normalization regarding the network size allows to compare different approaches even if the network sizes are different. The RMS is meanwhile being frequently used for evaluating self-localization systems.

$$\mathrm{RMS} = \sqrt{\frac{\sum_{i,j:i<j} \widehat{e}_{ij}^2}{N(N-1)\frac{1}{2}}} \tag{7}$$

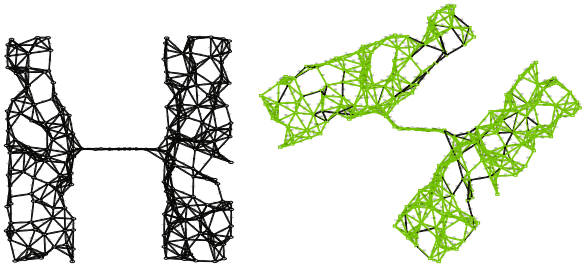

(a) (b)

**Fig. 3.** Simulation of an H-shaped network

### 3.2 Area Based Metrics

During our tests we made an interesting observation: Positioning errors are mainly located at the border of the network. Furthermore, they usually become detectable at the borders by deformations, e.g. parts of the network are folded in. This phenomenon is called *flip ambiguity*[12]. Nodes connect to previously flipped ones and propagate the error. The result are large virtually overlapping parts of the network which are causing large estimation errors. For a more detailed analysis of this major problem in localization please refer to the work of Kannan et al. [12]. Inside the network, the connectivity is higher and localization failures mainly accrue in areas with low connectivity. The probability for node misplacements inside of the system is low.

Analyzing localization systems described in the literature, we see that in most cases the deployment of sensor nodes is not relying on globally exact positioning of the individual nodes but on coverage. The exact distance estimation between two far away nodes (e.g., across the whole network) based on the virtual coordinate representation $p_v(\cdot)$ is mostly superfluous. Most location based services, as our client localization (step 3 in Figure 1), rely on accurate local position estimations and can absorb long range distance errors. The same holds for many other wireless applications. Thus, small local localization errors which may result in slight deformations of the virtual representation $p_v(\cdot)$ can be tolerated in most cases as long as the system makes sure that there is no overlapping of different network parts.

As an example, we investigated an H-shaped network as depicted in Figure 3 with a small bottleneck between two mass regions. Figure 3a shows the ground truth $p_r(\cdot)$. The bottleneck in this network is the very thin junction between the masses. Within this bottleneck, the probability for localization errors strongly increases. There is a high probability that this connection get bent in the virtual coordinate system $p_v(\cdot)$ as shown in Figure 3b. Table 1 shows the numerical results of this simulation.

Using the previously described distance metrics, the result shown in Figure 3b would be rated very poor. This happens, because these metrics synthesize a fully connected graph $G = (V, E_{all})$ and compare all the nodes with each other in the entire network regardless of their actual connectivity $E$. However, as can be seen,

**Table 1.** Metric results of Figure 3

| Simulation of an H-shaped network | |
|---|---|
| Left side RMS: | $3.659 \times 10^{-4}$ |
| Right side RMS: | $4.796 \times 10^{-4}$ |
| Overall RMS: | $1.204 \times 10^{-1}$ |
| AR (convex hull): | 96.38 % |
| AR (exact border): | 98.73 % |

the error is only high in a certain region. The overall RMS error for this example is $1.204 \times 10^{-1}$ (in total, 220 nodes have been used in this example), which is for our algorithm and in comparison to Figure 2b at least one order of magnitude too high. Using this metric would thus result in discarding the result.

However, if both masses are evaluated individually, the resulting RMSs would be $3.659 \times 10^{-4}$ and $4.796 \times 10^{-4}$, which are rather good results. The only problem is the bend in the middle. As stated before, in most cases, the following two conditions are relevant: First, the local accuracy for the localization service must be fulfilled (global accuracy, i.e. correct distance approximation of nodes far away from each other, is mostly negligible) and, secondly, parts of the network must not be overlapping to guarantee unique coordinates. The localization accuracy for the left as well as for the right masses are very good. Applications like location based routing or navigation in general work on the complete system as long as unique coordinates can be ensured. Based on the previous introduced metrics it is very had to get a clue whether parts of a network are overlapping or not.

In order to circumvent these problems, we introduce the Area Ratio (AR) as an area-based metric, which suits such non-uniform scenarios much better. AR brings both, the area of the ground truth $A_r$ and the area of the generated grid $A_v$ into relationship to each other as depicted in Equation 8.

$$\mathrm{AR} = \frac{A_v}{A_r} \tag{8}$$

The area of the covered real and the virtual ground can easily be computed by creating the convex hull over all nodes and, afterwards, computing the areas of the resulting polygons. We used the convex hull because our irregular simulation topologies were roughly formed like a round panel due to the absence of obstacles. Depending on the scenario, other techniques might be needed to (efficiently) find the borders of the network.

Figure 2c shows plots of our simulation results of the obstacle-less simulations. The values are more intuitive as from other metrics as they purely reflect the covered ground ratio. In this plot, differently to the previously plotted results for the distance based metrics, 1 (100 %) equals to perfect coverage.

Using the 220 node network shown in Figure 3b as an example, the AR using the convex hull for building the polygon gives an accuracy of 96.38 %. The convex

**Table 2.** Decision table for the appropriate metric approach

| Network size | constant | variable | | |
|---|---|---|---|---|
| Required distance accuracy | global | local (but unique) | | global |
| Obstacles | any | w/o | w/ | any |
| GER | X | - | - | - |
| RMS / GDE / ARD | X | O | - | X |
| AR (convex hull) | O | X | O | O |
| AR (exact border) | O | X | X | O |

("X" → useable; "O" → use with care; "-" → do not use)

hull cannot fully cover the complexity of this specific shape, thus, the results might be too pessimistic. Using the exact borders of the shapes an accuracy of 98.73 % can be stated. Obviously, this value provides more realistic results compared to a distance based metrics such as the RMS metric.

The exact border of a representation $p_x$ can for instance be found as follows. For each intersection of two edge $E_{i,j} := (N_i, N_j)$ and $E_{s,t}$ of a representation $p_x$ a new vertex $N_{ij,st}$ is added to $V$. Its position $p_x(N_{ij,st})$ is located at the intersection of the edges. The original edges $E_{i,j}$ and $E_{s,t}$ get removed from $E$ and new edges from $N_i$, $N_j$, $N_s$ and $N_t$ to $N_{ij,st}$ get inserted. Therefore in the representation $p_x$ every intersection of edges gets removed. Subsequently an arbitrary vertex $N_b$ located on the border of the graph representation $p_x$ had to be found. The final polygon for the area computation can be found by following this border until vertex $N_b$ is reached again.

## 4 Conclusions

In this paper, we discussed the need for comprehensive metrics for evaluating the quality of self-localization systems. We briefly reviewed the metrics available in the literature. First, we described a class of distance based metrics, the best known examples being GER and RMS. However, only the RMS provides the demanded capabilities for comparing the localization quality assuming different network sizes. We also discussed the quality and the problems of those metrics in general. In a second step, we presented an area-based metric that better fits the needs for estimating the localization quality in a local context.

Based on simulation results, we outlined the capabilities and limitations of these approaches. Depending on the application requirements, an appropriate evaluation metric has to be chosen. We conclude that the RMS metric should be used for evaluation if a global accuracy is required. If local accuracy is more important, e.g. for customer localization or information forwarding, results based on the RMS might be misleading. Instead, an area-based metric should be preferred. Table 2 summarizes our findings. It can be considered a conceptual matrix for selecting adequate metrics.

## References


1. Ahmed, A.A., Shi, H., Shang, Y.: SHARP: A New Approach to Relative Localization in Wireless Sensor Networks. In: 25th IEEE International Conference on Distributed Computing Systems (ICDCS 2005), 2nd International Workshop on Wireless Ad Hoc Networking (WWAN 2005), pp. 892–898. IEEE, Columbus (2005)
2. Akyildiz, I.F., Kasimoglu, I.H.: Wireless Sensor and Actor Networks: Research Challenges. Elsevier Ad Hoc Networks 2, 351–367 (2004)
3. Bulusu, N., Estrin, D., Girod, L., Heidemann, J.: Scalable Coordination for Wireless Sensor Networks: Self-Configuring Localization Systems. In: 6th International Symposium on Communication Theory and Applications (ISCTA 2001). Ambleside, Lake District (July 2001)
4. Dressler, F.: Self-Organization in Sensor and Actor Networks. John Wiley & Sons, Chichester (December 2007)
5. Eckert, J., Dressler, F., German, R.: Real-time Indoor Localization Support for Four-rotor Flying Robots using Sensor Nodes. In: IEEE International Workshop on Robotic and Sensors Environments (ROSE 2009), pp. 23–28. IEEE, Lecco (November 2009)
6. Eckert, J., German, R., Dressler, F.: An Indoor Localization Framework for Four-rotor Flying Robots Using Low-power Sensor Nodes. IEEE Transactions on Instrumentation and Measurement 60(2) (to appear, 2010)
7. Eckert, J., Koeker, K., Caliebe, P., Dressler, F., German, R.: Self-localization Capable Mobile Sensor Nodes. In: IEEE International Conference on Technologies for Practical Robot Applications (TePRA 2009), pp. 224–229. IEEE, Woburn (November 2009)
8. Eckert, J., Villanueva, F., German, R., Dressler, F.: A Self-Organizing Localization Reference Grid. In: 16th ACM International Conference on Mobile Computing and Networking (MobiCom 2010), Poster Session. ACM, Chicago (September 2010)
9. Girod, L.D.: A Self-Calibrating System of Distributed Acoustic Arrays. Phd thesis, University of California (December 2005)
10. Gotsman, C., Koren, Y.: Distributed Graph Layout for Sensor Networks. In: Pach, J. (ed.) GD 2004. LNCS, vol. 3383, pp. 273–284. Springer, Heidelberg (2005)
11. Howard, A., Mataric, M.J., Sukhatme, G.: Relaxation on a Mesh: a Formalism for Generalized Localization. In: IEEE/RSJ International Conference on Intelligent Robots and Systems (IROS 2001), Maui, HI, pp. 1055–1060 (October 2001)
12. Kannan, A.A., Fidan, B., Mao, G.: Analysis of Flip Ambiguities for Robust Sensor Network Localization. IEEE Transactions on Vehicular Technology 59(4), 2057–2070 (2010)
13. Liu, J., Zhang, Y., Zhao, F.: Robust Distributed Node Localization with Error Management. In: 7th ACM International Symposium on Mobile Ad Hoc Networking and Computing (ACM Mobihoc 2006), Florence, Italy (May 2006)
14. Mao, G., Fidan, B. (eds.): Localization Algorithms and Strategies for Wireless Sensor Networks. Idea Group Inc. (IGI), USA (2009)
15. Priyantha, N.B., Balakrishnan, H., Demaine, E., Teller, S.: Anchor-Free Distributed Localization in Sensor Networks. Tech. Rep. TR-892, MIT Laboratory for Computer Science (April 2003)
16. Xiao, J., Ren, L., Tan, J.: Research of TDOA Based Self-localization Approach in Wireless Sensor Network. In: IEEE/RSJ International Conference on Intelligent Robots and Systems (IROS 2006), pp. 2035–2040. IEEE, Beijing (October 2006)

## A Plausibility of the AR Metric

It is clear that two different graph representations $p_1, p_2$ with the same vertex set $V$ and edge set $E$ that have equal areas are not necessarily identically looking. However, at least in the field of self-localization (where distances, positions, and/or angles are known), it holds that if two graph representations have similar areas, they are similarly shaped. Taking this into account, the AR (Equation 8) can only be meaningful if the following assumption holds for the entire connected graph as well as for the majority of its sub-graphs:

$$A_v \leq A_r \tag{9}$$

Under the following conditions we can show that Equation 9 is violated with a probability of $P_{violate} < 0.5$ for two neighboring triangles:

- If $\|p(N_a) - p(N_b)\|_2 < R$ then $(N_a, N_b) \in E$
- $\epsilon_{i,j}$ of Equation 2 is negligible small if $(N_i, N_j) \in E$
- No three connected nodes that are placed collinear

Exploding this entity and increasing the number of vertexes to infinity ($|V| \to \infty$ or a sufficiently large number), Equation 9 holds for the entire system.

Self-localization is usually a 2-dimensional problem. Thus, the area of a node $N_a$ in which another node $N_b$ can connect to is defined by:

$$A^A := \{\boldsymbol{x} \in \Re^2 \mid \|p(N_a) - \boldsymbol{x}\|_2 < R\} \tag{10}$$

Due to the described restriction, flipped areas can only occur if the connectivity of a newly joined node $N_f$ is $d(N_f) = 2$. Let previously localized nodes be $N_a$ and $N_b$. The possible placement $p(N_f)$ for the node $N_f$ is within:

$$A^{AB} := \{\boldsymbol{x} \in \Re^2 \mid A^A \cap A^B\} \tag{11}$$

Now, let $N_c \in A^{AB}$ be a third node. As depicted in Figure 4, the nodes $N_a, N_b, N_c$ are forming the triangle $\triangle ABC$. The virtual as well as truth graph representation ($p_v(\cdot)$ and $p_r(\cdot)$, respectively) must have the same areas. Without loss of generality we define the x-values of node $N_a$ and node $N_b$ to 0:

$$p(N_i) := (0, y_i)^T;\ i \in \{a, b\} \tag{12}$$

Thereby, two subsets $A_+$ and $A_-$ representing the positive and the negative plane, respectively, are separated by the line $\overline{AB}$. A new node $N_f$ can only be flipped if it is not connected to node $N_c$. This possible area is defined as:

$$A^{AB\backslash C} := \{\boldsymbol{x} \in \Re^2 \mid (A^A \cap A^B)\backslash A^C\} \tag{13}$$

A *bad* situation (the inverse of Equation 9) can only happen if for the ground truth representation $p_r(\cdot)$ the sign of the y-axis of the node $N_c$ is the same as of node $N_f$ ($sgn(y_f) = sgn(y_c)$). The resulting intersection of line $\overline{AC}$ and line $\overline{BF}$ is called $D$. If the virtual representation $p_v(N_f)$ for node $N_f$ is flipped to $p_v(N_{f'})$

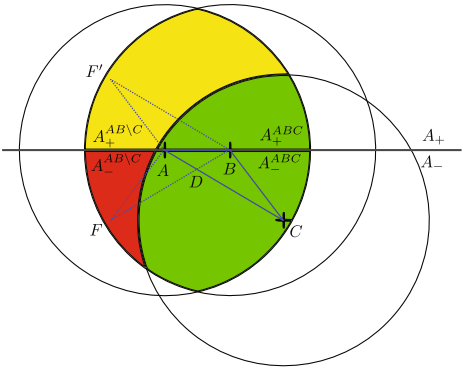


**Fig. 4.** Flip scenario

as depicted in Figure 4, Equation 9 does not hold. The area of the polygons can be calculated as follows:

$$A^{ABCDF} = A^{\triangle ABC} + A^{\triangle ABF} - A^{\triangle ABD} \tag{14}$$

$$A^{AF'BC} = A^{\triangle ABC} + A^{\triangle ABF'} \tag{15}$$

Note that $A^{\triangle ABF} = A^{\triangle ABF'}$. Thus, it can be easily seen that Equation 9 does not hold:

$$A_r = A^{ABCDF} < A^{AF'BC} = A_v \tag{16}$$

If we assume a worst case flip probability of $P_{flip} = 0.5$ (if no additional knowledge is present), then the probability of violating Equation 9 can be given as:

$$P_{violate} = \frac{A_-^{AB\backslash C}}{A^{AB\backslash C}} < 0.5 \tag{17}$$

Whereas $A_-^{AB\backslash C} = A^{AB\backslash C} \cap A_-$ and $A^{AB\backslash C} = A_+^{AB\backslash C} \cup A_-^{AB\backslash C}$ ($A_+^{AB\backslash C} \cap A_-^{AB\backslash C} = \emptyset$).

We now show that the following equation always holds:

$$A_-^{AB\backslash C} < A_+^{AB\backslash C} \tag{18}$$

Thus, the probability of placing a new node into $A_-^{AB\backslash C}$ (instead of $A_+^{AB\backslash C}$) is less then $P_{violate} < 0.5$. If this experiment is repeated for a sufficient number of nodes, the probability that Equation 9 hold is $\lim_{N\to\infty} P_{Eq9} \to 1$.

Suppose $p_r(N_c) \in A_-$; $p_r(N_c) \in A_+$ can be shown analog. The area $A^{AB}$ is symmetrical to the line $\overline{AB}$ which is equal to the x-axis. Thereby (due to the symmetry property):

$$A^C \cap A_- > A^C \cap A_+ \tag{19}$$

due to $p_r(N_c)_y < 0$. Thus:

$$A^{ABC} \cap A_- > A^{ABC} \cap A_+ \tag{20}$$

By migrating to the complimentary follows Equation 18 (*q.e.d.*).